NASA-CR-191247

P- 10

FINAL REPORT TO THE

NATIONAL AERONAUTICS AND SPACE ADMINISTRATION

ON RESEARCH SUPPORTED BY GRANT NAG3-993:

MODELING OF COALESCENCE, AGGLOMERATION AND PHASE SEGREGATION IN MICROGRAVITY PROCESSING OF BIMETALLIC COMPOSITE MATERIALS

Name and Address of Institution:

The Regents of the University of Colorado
Campus Box 19
Boulder, CO 80309-0019

Time Period of Support:

2/2/89-9/30/92

Principal Investigator:

Robert H. Davis, Professor
Department of Chemical Engineering
University of Colorado
Boulder, CO 80309-0424
Telephone: (303) 492-7314

Responsible NASA Official:

R. Balasubramanian
Mail Stop 500-217
NASA Lewis Research Center
21000 Brookpark Road
Cleveland, OH 44135
Telephone: (216) 433-2878

Date of Final Report:

11/10/92

Summary of Technical Progress

Objectives: The overall objective of this research is to develop models to predict drop-size-distribution evolutions due to droplet collisions and coalescence during processing within the miscibility gap of bimetallic liquid-phase-miscibility-gap materials. The individual and collective action of gravitational and nongravitational mechanisms on the relative motion and coalescence of drops are considered.

Research Task Description: When bimetallic liquid-phase-miscibility-gap materials, which are thought to have a variety of desirable properties, are cooled through the miscibility gap, droplets rich in one of the metals form in the liquid matrix rich in the other metal. Droplet coalescence and phase segregation then occur due to buoyancy and to thermocapillary and other nongravitational mechanisms. In order to gain a predictive understanding of these phenomena, population dynamics models are used to follow drop-size distribution evolutions in time as the droplets grow due to collisions and coalescence. Continuous drop size distributions are discretized into a large number of categories. Drops of a given mass are destroyed by coalescing with other drops and are formed by the coalescence of smaller drops. The population dynamics model tracks the formation and destruction of drops in each size category.

The relative motion of drops which gives rise to their collision and coalescence is considered to occur by gravity sedimentation, Marangoni migration, Brownian motion, and bulk flow. These collision mechanisms are considered either individually or collectively in the population dynamics models. In general, different mechanisms dominate for different processing conditions, materials properties, and drop-size ranges.

The collision kernals appearing in the population dynamics models require expressions for the collision rate between drops of two different sizes. Classical expressions attributed to Smoluchowski are improved to include attractive, repulsive, and hydrodynamic interactions between drops. In particular, trajectory calculations are used to predict collision efficiencies, which represent the ratio of the collision rate with these interactions to the Smoluchowski collision rate without these interactions, as functions of the size ratio, viscosity ratio, and other relevant dimensionless parameters.

Accomplishments: During the three years of NASA support, the following progress was made:

1. A computer program has been completed for solving the population dynamics model to follow droplet size evolutions with time in homogeneous dispersions due to collisions arising from gravity sedimentation, Marangoni migration, and/or Brownian motion. Some of the key results are that a bimodal initial distribution will exhibit much more rapid coalescence due to gravity sedimentation or Marangoni migration than will a unimodal initial distribution (Figure 1), a unimodal initial distribution will evolve into a bimodal distribution and then into a shifted and broadened unimodal distribution (Figure 2), and that coalescence may be greatly reduced by antiparallel alignment of the gravity vector and the temperature gradient (Figure 3).

2. Collision efficiencies for Brownian motion (Figure 4) and gravity sedimentation (Figure 5) for drops having a range of viscosity and radius ratios have been computed both in the presence and absence of attractive forces. A key result is that, in contrast to rigid particles, spherical liquid drops have nonzero collision efficiencies in the absence of attractive forces.

3. Theoretical work has been completed to predict collision efficiencies for Marangoni migration of two drops of different sizes in a temperature gradient Example results are shown in Figure 6. Note that the collision efficiencies for thermocapillary motion are larger than those for gravity motion, because of the more rapid decay of the velocity fields created by drops undergoing thermocapillary motion, provided that

the thermal conductivity of the drops is not too large. Surprisingly, however, the relative mobility function along the line-of-centers can become negative for large thermal conductivities (Figure 7), indicating that the smaller drop moves away from the larger drop and that there is a region of closed trajectories which prevents coalescence in the absence of attractive forces (Figure 8).

4. In related experimental work, drop size distributions of butyl benzoate in water are followed with time by holography as coalescence occurs due to gravity motion. We are also examining the interaction of two drops with video microscopy. An example of coalescence is shown in Figure 9, and measured relative trajectories of two drops are shown in Figure 10 to be in good agreement with theory.

5. Theoretical work on combined mechanisms for drop coalescence has been focused on buoyancy and Marangoni motion with the gravity vector aligned parallel or antiparallel to the temperature gradient. Our results show that there is a finite region in parameter space for which no collisions occur (Figure 11). This is because the interaction of two drops due to thermocapillary migration decays more rapidly (as $1/r^3$) with the separation distance (r) than does the interaction of two drops in gravity motion (which decays as $1/r$). As a result, the large drop which moves toward a small drop below it due to gravity may reach a separation distance where the initially weaker thermocapillary effects just balance the buoyancy-driven relative motion, and so the separation distance would then no longer decrease (Figure 12). With appropriate antiparallel alignment of buoyancy and Marangoni velocities, a polydisperse suspension of small drops is predicted to evolve into a monodisperse suspension of larger drops (Figure 13).

6. Time scales have been determined for phase segregation and drop coalescence, together with criteria for predicting whether or not significant coalescence will occur prior to phase segregation. A computer model has been developed to solve population balances for drop size distributions which vary in space due to buoyancy or thermocapillary motion. Results show that the phase segregation rate initially increases due to coalescence and subsequently decreases as the larger drops migrate out of suspension (Figure 14).

7. Physical data on a variety of bimetallic and transparent immiscibles have been collected, and dimensionless parameters representing various effects have been tabulated as functions of drop size. Data on composite Hamaker constants (for van der Waals attractions) and temperature coefficients of interfacial tension (for thermocapillary migration) are sparse, and order-of-magnitude estimates are typically used. Calculations of collision efficiencies have been made for bismuth drops in a zinc melt, for ethyl salicytate drops in diethylene glycol, and for lead drops in an aluminum melt.

Publications

Barnocky, G. and Davis, R.H., "The Lubrication Force Between Spherical Drops, Bubbles and Rigid Particles in a Viscous Fluid," *Int. J. Multiphase Flow* **15**, 627-638 (1989).

Davis, R.H., Schonberg, J.A., and Rallison, J.M., "The Lubrication Force Between Two Viscous Drops," *Phys. Fluids A* **1**, 77-81 (1989).

Rogers, J.R. and Davis, R.H., "Modeling of Coalescence in Microgravity Processing of Zn-Bi Immiscible Alloys," *Met. Trans. A.* **21**, 59-68 (1990).

Rogers, J.R. and Davis, R.H., "The Influence of van der Waals Attractions on Cloud Droplet Growth by Coalescence," *J. Atmos. Sci.* **47**, 1075-1080 (1990).

Yiantsios, S.G. and Davis, R.H., "On the Buoyancy Driven Motion of a Drop Towards a Rigid Surface or a Deformable Interface," *J. Fluid Mech.* **217**, 547-573 (1990).

Zhang, X. and Davis, R.H., "The Rate of Collisions of Viscous Drops Due to Gravity or Brownian Motion," *J. Fluid Mech.* **230**, 479-504 (1991).

Yiantsios, S.G. and Davis, R.H., "The Deformation of Two Unequal Drops in Near-Contact Buoyancy Driven Motion," *J. Colloid Interface Sci.* **144**, 412-433 (1991).

Rogers, J.R., *Experimental and Modeling Studies of Droplet Growth Due to Coalescence*, PhD Thesis, University of Colorado (1991).

Zhang, X. and Davis, R.H., "Collision Efficiencies of Small Drops," *Proc. Chinese Acad. Sci. Workshop* (1991).

Zhang, X. and Davis, R.H., "The Collision Rate of Small Drops Undergoing Thermocapillary Migration," *J. Colloid Interface Sci.* **152**, 548-561 (1992).

Davis, R.H., Zhang, X., and Wang, H., "Hydrodynamics of Dispersions and Coagulation," *Proc. Int. Workshop on Systems with a Miscibility Gap* (ed. L. Ratke), Bad Honnef, Germany, 157-174 (1992).

Zhang, X., *Relative Motion, Collision and Coalescence of Small Spherical Drops*, PhD Thesis, University of Colorado (1992).

Zhang, X., Davis, R.H., and Ruth, M.F., "Experimental Study of Two Interacting Drops in an Immiscible Fluid," *J. Fluid Mech.* (in press).

Wang, H. and Davis, R.H., "Droplet Growth due to Brownian, Gravitational, or Thermocapillary Motion and Coalescence in Dilute Dispersions," *J. Colloid Interface Sci.* (under review).

Zhang, X., Wang, H., and Davis, R.H., "Collective Effects of Temperature Gradients and Gravity on Droplet Coalescence," *Phys. Fluids A* (under review).

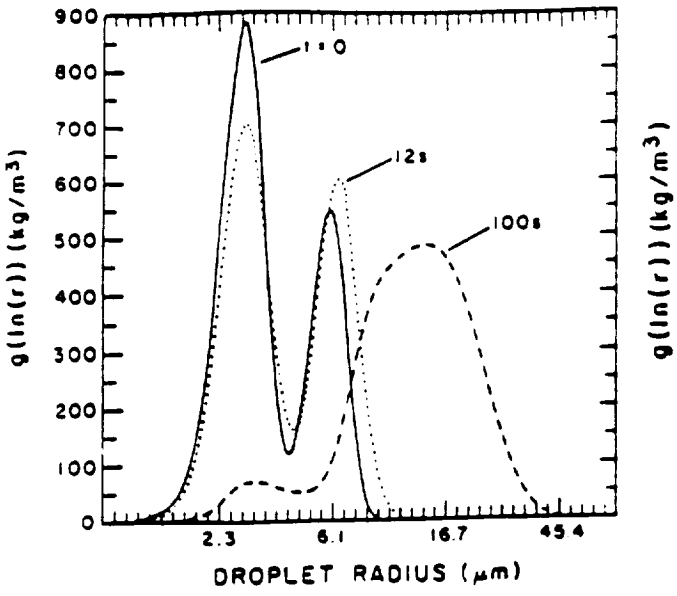

Figure 1a. Time evolution of the drop size distribution for a bimodal initial distribution of bismuth drops undergoing Marangoni migration in molten zinc.

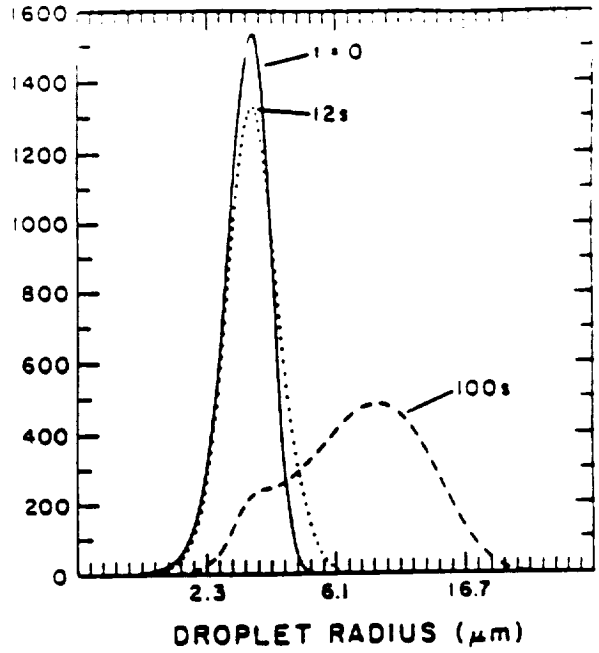

Figure 1b. Time evolution of the drop size distribution for a unimodal initial distribution of bismuth drops undergoing Marangoni migration in molten zinc.

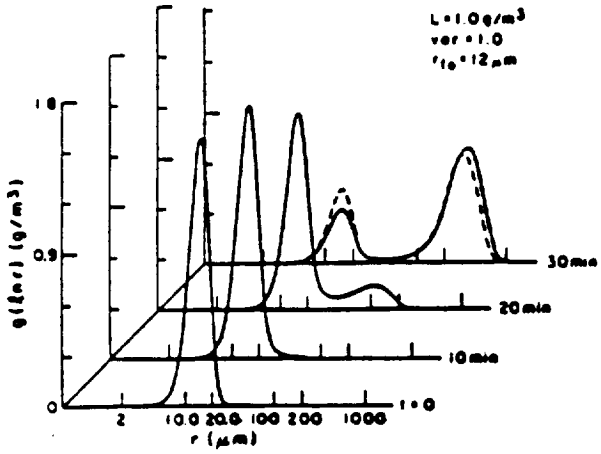

Figure 2. Time evolution of the drop size distribution for a unimodal initial distribution of water drops subject to gravity sedimentation in air.

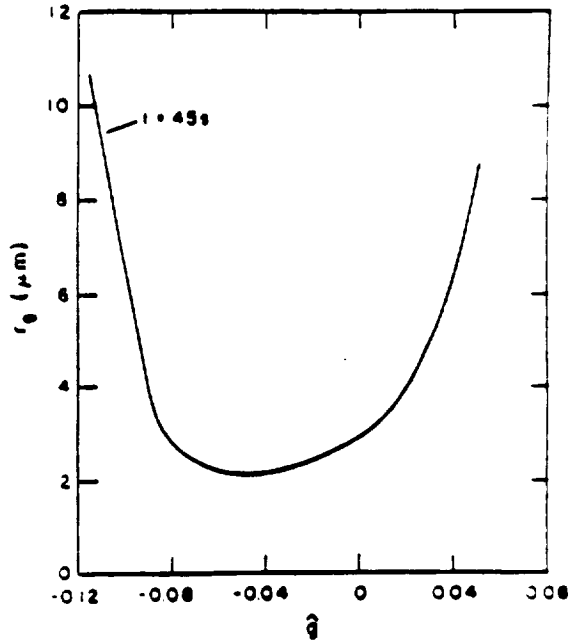

Figure 3. Mass average drop radius at t=45 seconds due to combined gravity and Marangoni motion of bismuth drops in zinc as a function of gravity strength relative to normal for parallel ($\hat{g} > 0$) and antiparallel ($\hat{g} < 0$) orientation of gravity vector and temperature gradient. The initial mass average radius is r_g=2 μm.

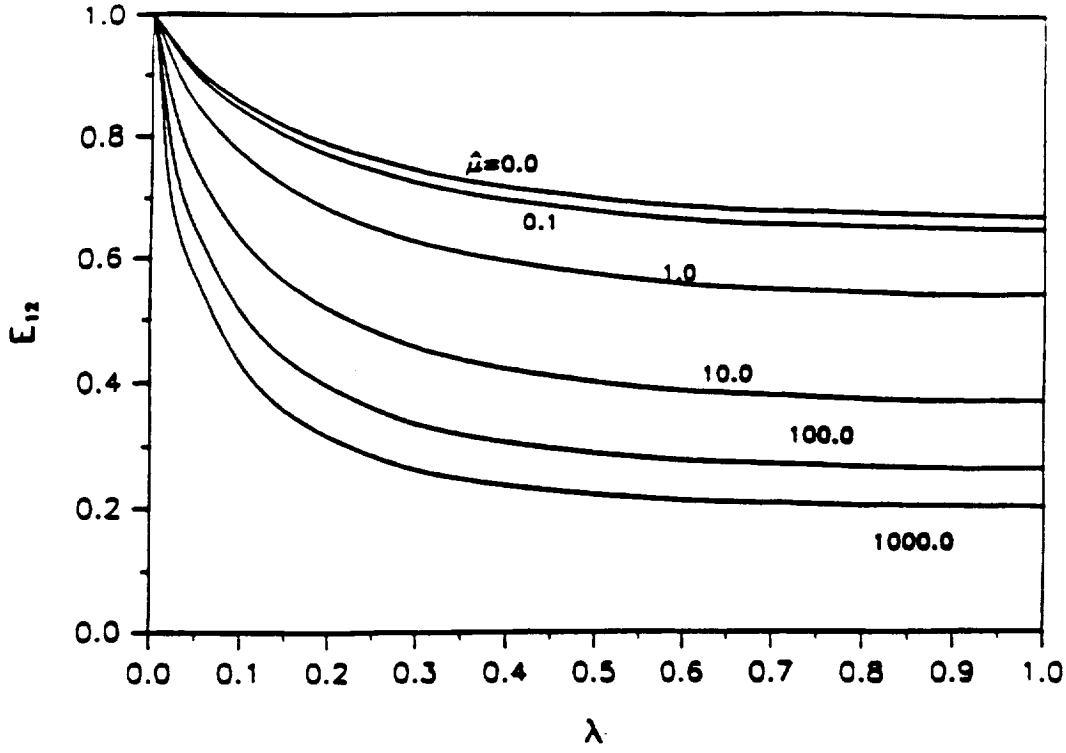

Figure 4. **Collision efficiencies for viscous drops of various viscosity ratios ($\hat{\mu}$) and size ratios (λ) undergoing Brownian motion in the absence of attractive forces.**

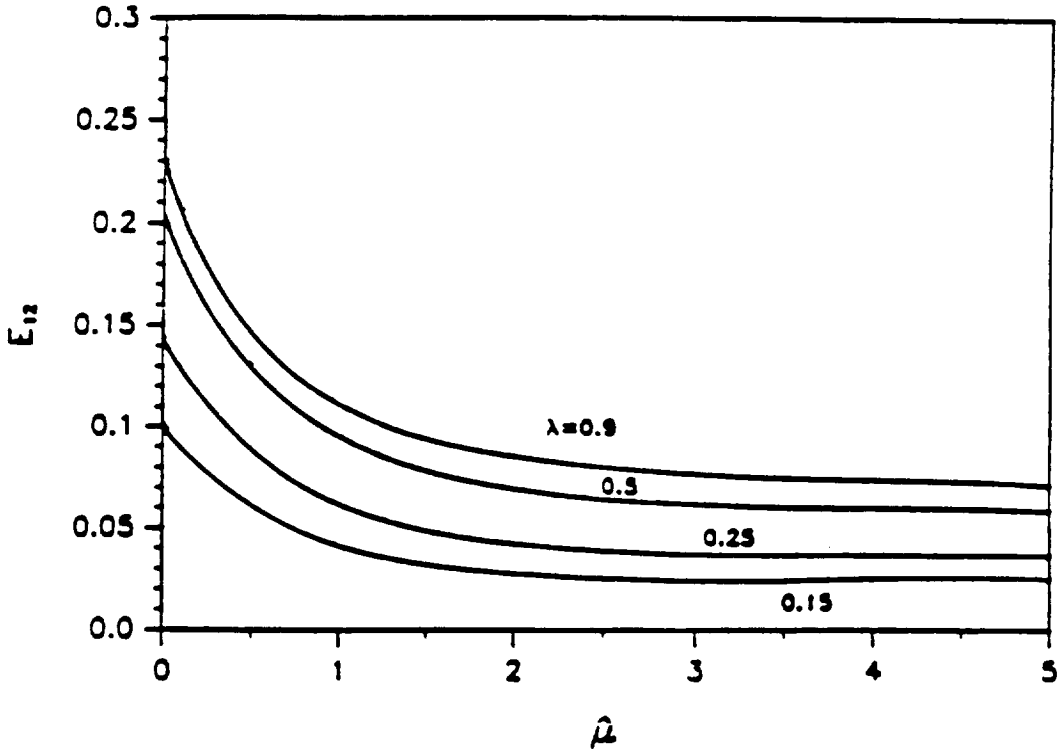

Figure 5. **Collision efficiencies for viscous drops of various size ratios (λ) and viscosity ratios ($\hat{\mu}$) undergoing gravity sedimentation in the absence of attractive forces.**

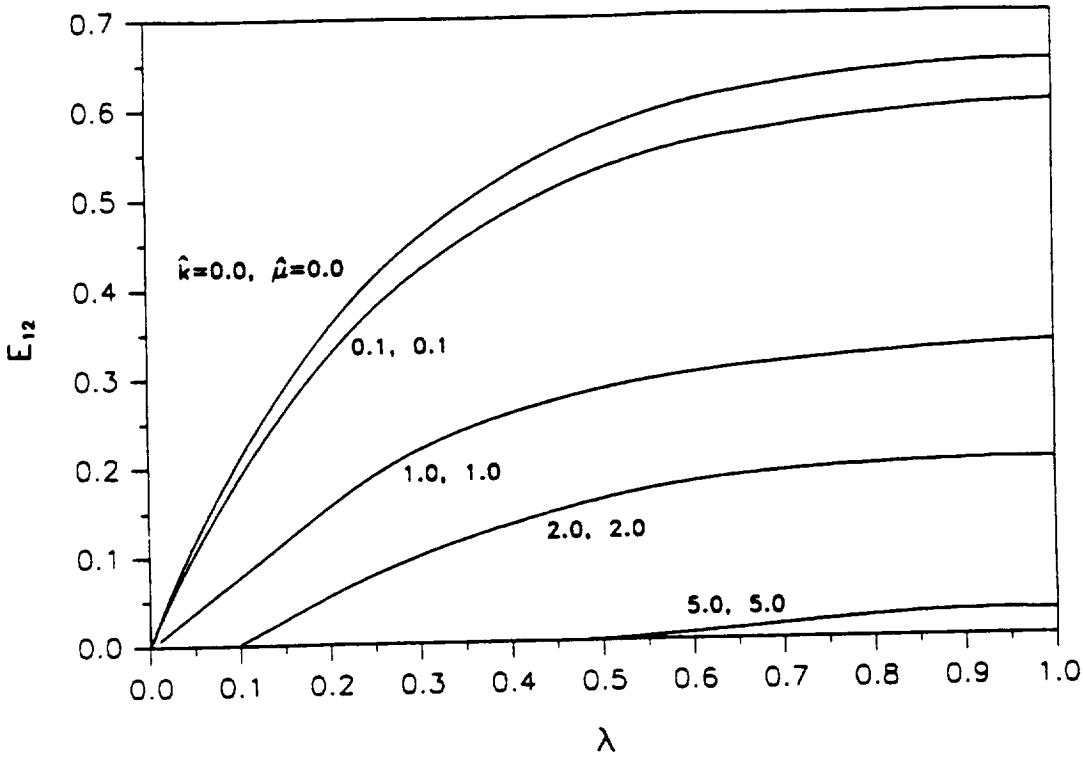

Figure 6. **Collision efficiencies as a function of the drop size ratio (λ) for drops of various thermal conductivity ratios ($\hat{\kappa}$) and viscosity ratios ($\hat{\mu}$) undergoing thermocapillary migration in the absence of attractive forces.**

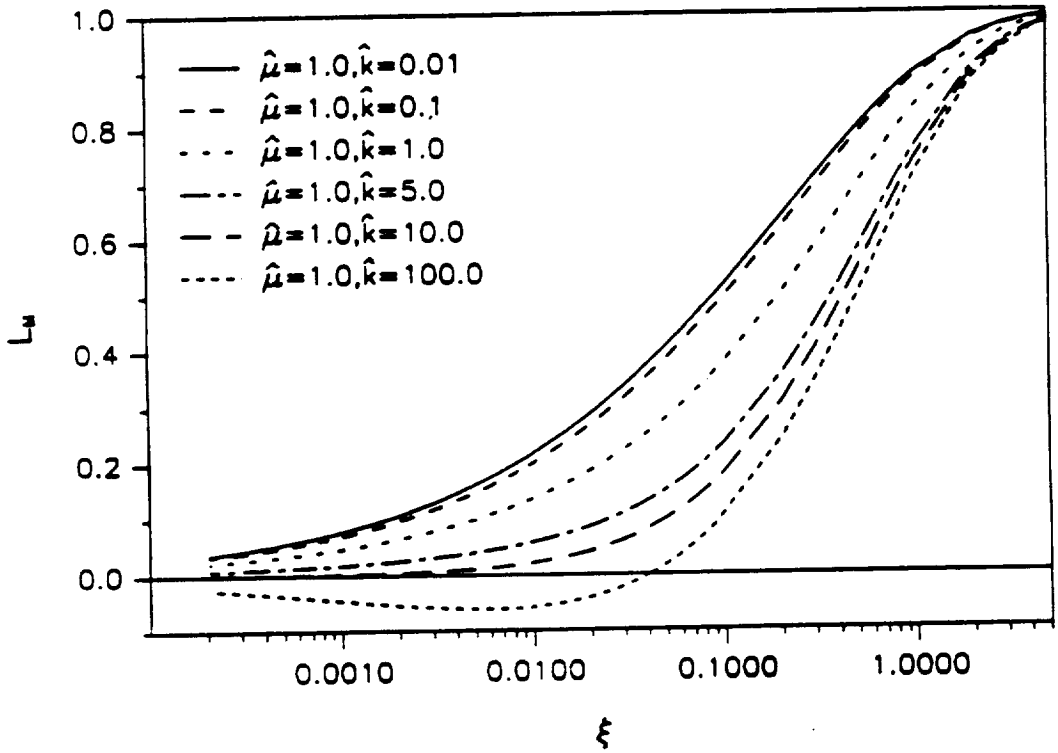

Figure 7. **Relative mobility function versus the dimensionless separation distance for two unequal drops (λ = 0.5) in relative motion along their line of centers due to thermocapillary migration, for various thermal conductivity ratios ($\hat{k}$) and viscosity ratios ($\hat{\mu}$).**

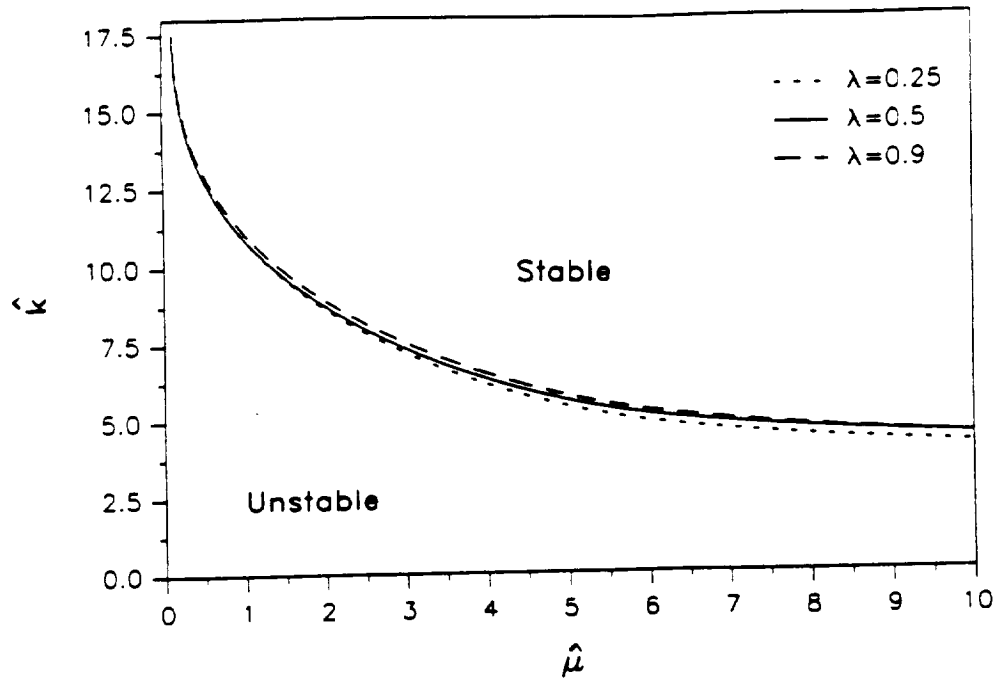

Figure 8. **Stability diagram showing regions of no collisions (stable) and collisions (unstable) for two spherical drops undergoing thermocapillary migration in the absence of attractive forces.**

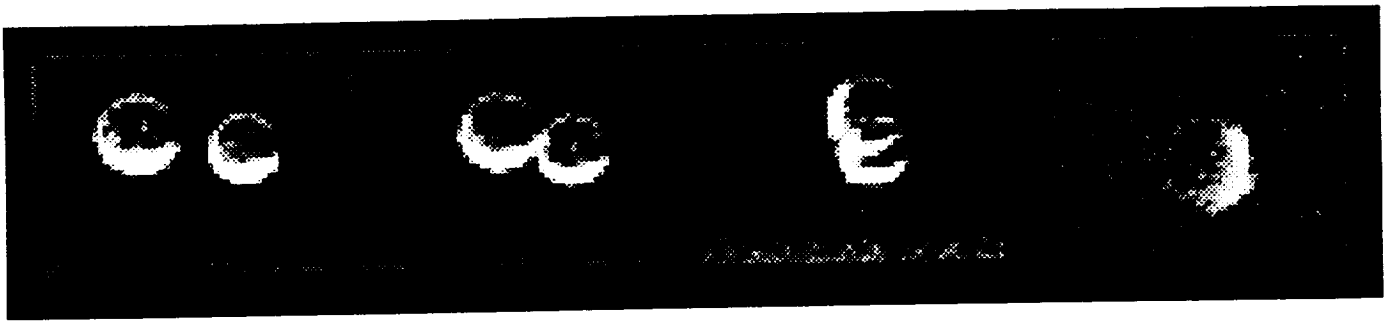

t = 0 sec t = 3 sec t = 10 sec t = 17 sec

Figure 9. **Time sequence of approach and coalescence due to gravity of two castor oil drops in a silicon fluid.**

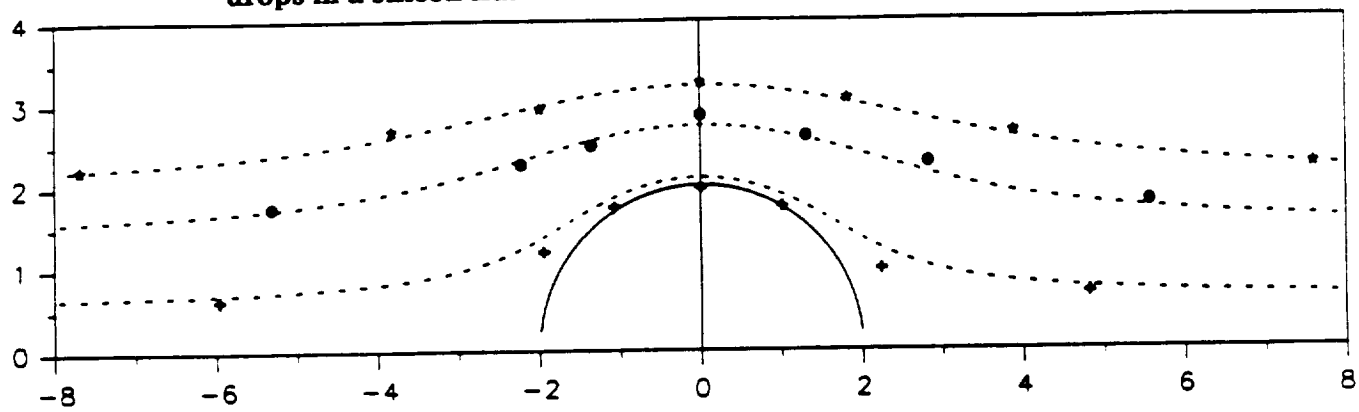

Figure 10. **Dimensionless relative trajectories of two different sized castor oil drops moving due to gravity in a silicon fluid. The symbols are experimental data and the dashed lines are theory.**

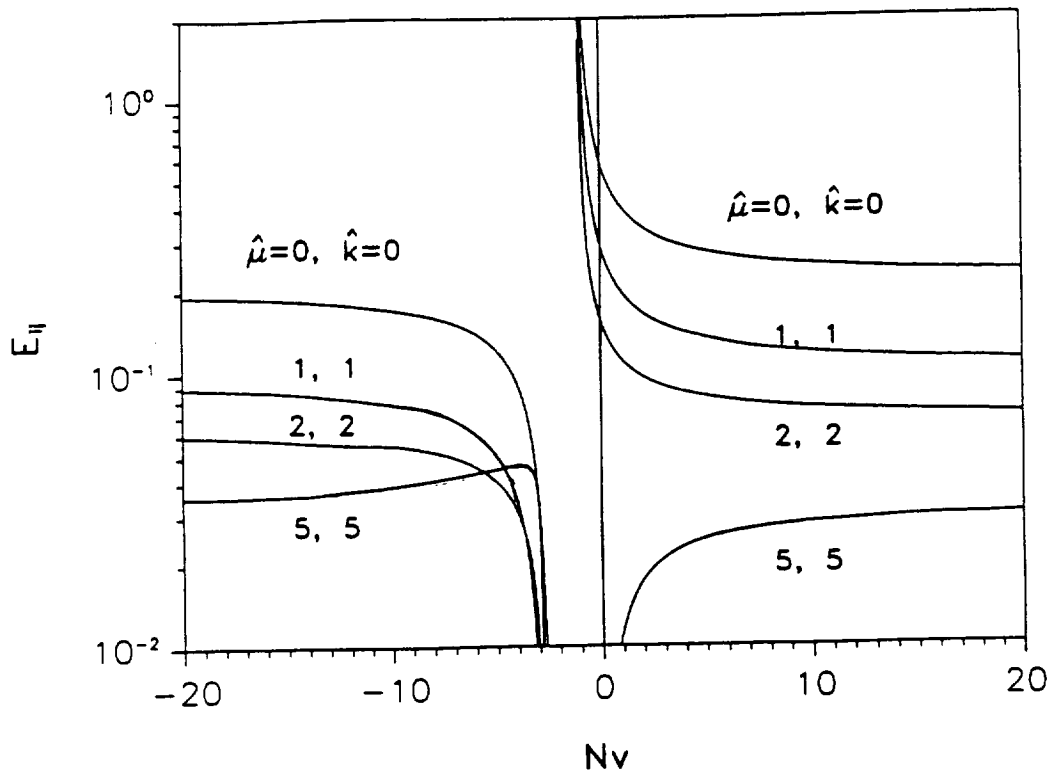

Figure 11. **The collision efficiency versus the ratio of buoyancy and thermocapillary relative velocities for two widely spaced drops of size ratio $\lambda = 0.5$ for various viscosity ($\hat{\mu}$) and thermal conductivity ratios ($\hat{k}$).**

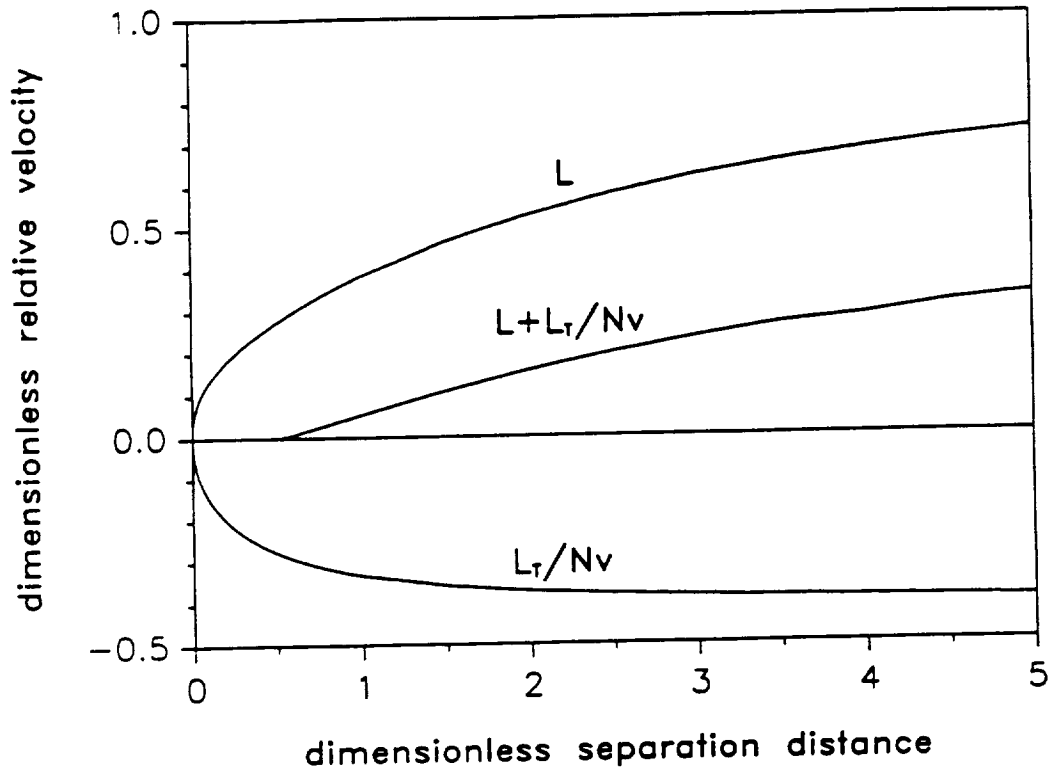

Figure 12. **The dimensionless gravitational (L), thermocapillary (L_T/N_v) and combined relative velocities versus separation distance for two drops with $\lambda = 0.5$, $\hat{\mu} = 1$, $\hat{k} = 1$, and $N_v = -2.5$.**

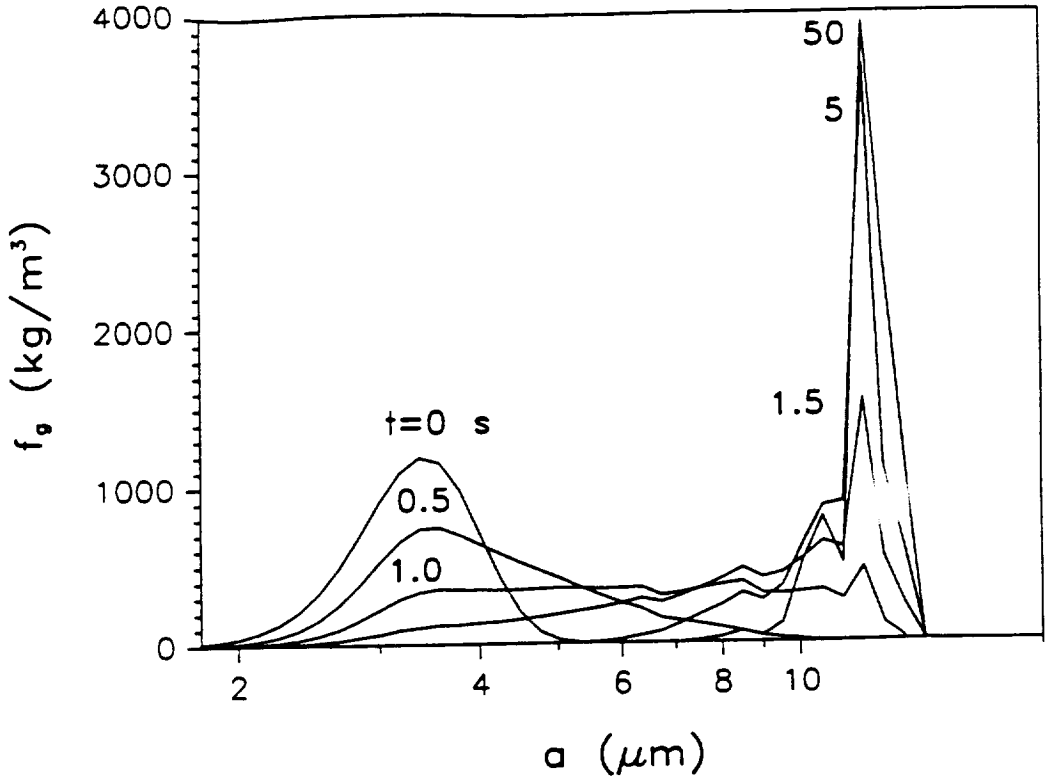

Figure 13. Evolution of the size distribution of lead drops in an aluminum melt for antiparallel alignment of the gravity vector (9.8 m/s^2) and temperature gradient (10^3 K/m).

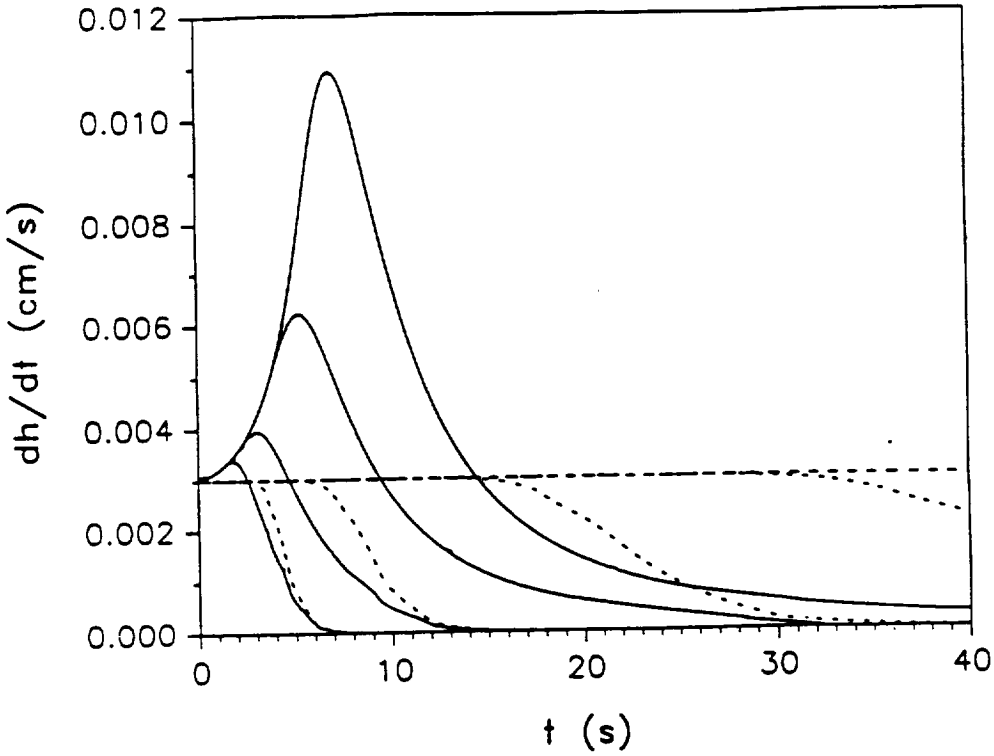

Figure 14. The rate of phase separation versus time for a dispersion of bismuth drops undergoing simultaneous buoyancy motion and coalescence in a zinc melt in containers of increasing height (left to right), the dashed curves are the corresponding results in the absence of coalescence.